

Optical processes in carbon nanocolloids

Giulio Ragazzon,^{1,*} Alejandro Cadranel,^{2,3,4} Elena V. Ushakova,^{5,6} Yichun Wang,^{7,8} Dirk M. Guldi,^{2,*} Andrey L. Rogach,^{5,6,9,*} Nicholas A. Kotov,^{7,8,10,11,12,*} and Maurizio Prato^{1,13,14,*}

SUMMARY

In recent years, carbon dots, graphene quantum dots, and other carbon nanocolloids have attracted a mounting interest as readily available, non-toxic, and tailorable carbon-based nanomaterials. One of the most fascinating features of carbon nanocolloids is their luminescence, the origin of which remains a source of dispute. The lack of understanding of the optical properties of carbon nanocolloids hampers their use in technological, environmental, and biomedical processes. Here, we review the current knowledge of excited states in carbon nanocolloids and related properties, inviting researchers to embrace the complexity of carbon nanocolloids. We point to the fundamental problems associated with their structure, photophysics, and photochemistry and highlight multiple directions of current and future research of this exciting class of nanomaterials.

INTRODUCTION

Carbon nanocolloids (CNCs) is the cumulative term that we will use here to refer to the plethora of dispersible nanoscale particles made predominantly from carbon atoms. They encompass nanostructures known as carbon dots, graphene quantum dots, carbon nanooxions, nanoscale carbon black, and other nanoscale carbon particles having typical dimensions below and around 10 nanometers.¹⁻³ They share a lot of properties, that have attracted mounting interest among scientists, such as the strong luminescence, low toxicity, water-solubility, ease of synthesis, high surface area, and the possibility to tune their optical properties.³ The fluorescence of CNCs is likely their most attractive optical feature, marking a strong difference with the common carbon-based nanomaterials, such as carbon nanotubes and microscale platelets of graphene and graphene oxide. Specifically, most CNCs display an excitation-dependent emission accompanied by large Stokes shifts that are uncommon among typical organic dyes. These properties have stimulated a broad interest and have been subject to intense investigation, however, a unifying picture is still lacking.⁴⁻⁶ Besides fluorescence, excited states of CNCs give rise to several optical processes with phosphorescence and chiroptical activity being the most prominent. Management of charge and photons in the excited state is also scientifically and technologically intriguing. Fundamental studies at the single-particle level and the exploitation of less common spectroscopic techniques will contribute to understanding the optical properties of CNCs. Here, we provide a tutorial review of the current knowledge of the optical properties of CNCs, including aspects that are less frequently discussed, such as chiroptical properties and phosphorescence. Representative examples of photon- and charge-management in the excited state are highlighted, and our vision on the opportunities arising from the versatility of CNC excited states is shared with the readers.

The bigger picture

Light is the original source of most energy on Earth, allowing us to see and live. It is also central to many technological processes. Therefore, innovative nanomaterials that can absorb, generate, or further exploit light are of utmost importance, having the potential to become pervasive in our lives. This is the case for carbon nanocolloids, which are ubiquitous, biocompatible, and inexpensive, which are the three important prerequisites for their broader application in different fields of technology. Yet, despite intense research for a number of years, a unifying picture describing the excited-state properties of these nanocolloids is lacking. It is possibly the time when this approach should be reversed, embracing the inherent diversity of excited states in carbon-based particles, which enable us to focus on engineering their optical properties based on their structural variability. A deeper understanding of the molecular features of carbon nanocolloids is emerging as one of the key factors, which will allow unlocking excited-state processes appearing out of reach, unfolding the full potential of optical processes in this potent family of nanomaterials.

Classification, synthesis, structure, and excited states

CNCs include a variety of sub-categories having different patterns of atomic connectivity and structural anisotropy. Although the boundaries between these categories are blurred, few main sub-categories can be identified, which are recurrent in the literature and present rather distinctive traits (Figure 1).⁷ At one end of the spectrum are amorphous polymeric structures with a minimum degree of carbonization, identified as carbonized polymer dots (CPDs). Structures with increased carbonization are referred to as carbon nanodots (CNDs), whereas multilayer stacks of graphitic sheets are typically referred to as carbon quantum dots (CQDs). Finally, nanometer-sized fragments of crystalline graphene with up to three layers stacked are identified as graphene quantum dots (GQDs), completing the range of possibilities.

The synthesis of CNCs typically requires rather harsh conditions, needed for the formation of new carbon-carbon bonds. Common precursors are small molecules undergoing decomposition, polymerization, and carbonization under hydrolytic, solvothermal, or pyrolytic conditions. Microwave irradiation of precursor solutions has also proven as an effective tool, providing much shorter reaction times.⁸ In these cases, the formation of CNCs likely proceeds through the formation of a polymeric structure, followed by incomplete carbonization at high temperature or prolonged times. A different scenario is observed in the so-called top-down synthesis, in which larger carbon structures are subject to ultrasonication, laser ablation, arc discharge, and electrochemical etching, effectively cutting larger carbon structures into smaller pieces.² The degree of control over the final nanostructures in these methods is typically lower compared with the one achieved using bottom-up methods.

In all cases, the detailed structure of these materials can vary significantly, even within the same category and within the same sample. A general consequence of this is that—in principle—the observed properties may arise from a small portion of the whole sample that is particularly active. The intrinsic diversity is indeed the reason why CNCs are better identified as a material, rather than precise molecular or nanoscale entities. Using an analogy taken from Nature, we might consider the variability of CNCs resembling that of enzyme families that display a rich variety of structures. Such an inherent diversity is a distinctive feature of CNCs and requires caution in drawing general conclusions from the study of a single or just a few materials. For the same reason, performing a careful and extensive material purification and characterization is critical to support specific claims and offers to the scientific community a solid basis to rationalize the observed behaviors.

When small molecules are used as precursors, dialysis is an ideal purification method, which could be coupled with filtration steps, to eliminate large carbonaceous side products. As recently discussed in detail elsewhere, membranes with appropriate molecular weight cutoff should be employed.⁹ Concerning the characterization, the evaluation of the size by transmission electron microscopy (TEM) and/or atomic force microscopy is required, although it is often not sufficient to prove the formation of CNCs. Indeed, these techniques require solvent evaporation, and with a concomitant concentration of the sample, it was observed that nanometer-sized aggregates could be detected even when analyzing small molecules.¹⁰ Such aggregates even displayed *d* spacing comparable with that of the graphite interlayer distance of about 0.33 nm. Dynamic light scattering has the potential to overcome this limitation, however, the small sizes and low scattering of CNCs make the use of this analytical technique challenging. To understand the nature of the formed material, X-ray photoelectron spectroscopy (XPS) is often employed and the results are very helpful to uncover the elemental composition and the

¹Department of Chemical and Pharmaceutical Sciences, University of Trieste, Via Licio Giorgieri 1, Trieste 34127, Italy

²Department of Chemistry and Pharmacy, Interdisciplinary Center for Molecular Materials, Friedrich-Alexander Universität Erlangen-Nürnberg, Egerlandstraße 3, 91058 Erlangen, Germany

³Universidad de Buenos Aires, Facultad de Ciencias Exactas y Naturales, Departamento de Química Inorgánica, Analítica y Química Física, Pabellón 2, Ciudad Universitaria, C1428EHA Buenos Aires, Argentina

⁴CONICET – Universidad de Buenos Aires, Instituto de Química-Física de Materiales, Medio Ambiente y Energía (INQUIMAE), Pabellón 2, Ciudad Universitaria, C1428EHA Buenos Aires, Argentina

⁵Center of Information Optical Technologies, ITMO University, 49 Kronverksky Pr., Saint Petersburg 197101, Russia

⁶Department of Materials Science and Engineering, and Centre for Functional Photonics (CFP), City University of Hong Kong, 83 Tat Chee Avenue, Kowloon, Hong Kong SAR, P.R. China

⁷Biointerfaces Institute, University of Michigan, 2800 Plymouth Road, Ann Arbor, MI 48109, USA

⁸Department of Biomedical Engineering, University of Michigan, Ann Arbor, MI 48109, USA

⁹Shenzhen Research Institute, City University of Hong Kong, Shenzhen 518057, P.R. China

¹⁰Department of Chemical Engineering, University of Michigan, Ann Arbor, MI 48109, USA

¹¹Department of Materials Science, University of Michigan, Ann Arbor, MI 48109, USA

¹²Department of Macromolecular Science and Engineering, University of Michigan, Ann Arbor, MI 48109, USA

¹³Center for Cooperative Research in Biomaterials (CIC biomaGUNE), Basque Research and Technology Alliance (BRTA), Paseo de Miramón 182, 20014 Donostia-San Sebastián, Spain

¹⁴Basque Foundation for Science, Ikerbasque, Bilbao 48013, Spain

*Correspondence: gragazzon@units.it (G.R.), dirk.guldi@fau.de (D.M.G.), andrey.rogach@cityu.edu.hk (A.L.R.), kotov@umich.edu (N.A.K.), prato@units.it (M.P.)
<https://doi.org/10.1016/j.chempr.2020.11.012>

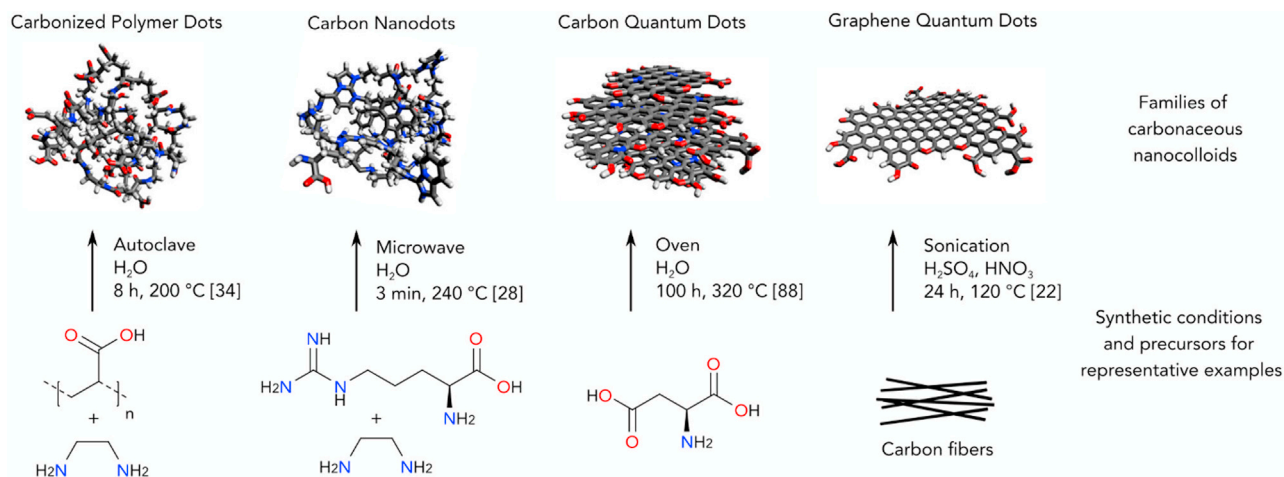


Figure 1. Representative carbon nanocolloids

Illustration of representative types of CNCs, with an increasing degree of sp^2 character from left to right, usually identified as CPDs, CNDs, CQDs, and GQDs. For each type of CNCs, the precursors and synthetic conditions of a representative member are presented here.

type of bonds present on the surface of CNCs. Considering the penetration depth of XPS analysis (a few nanometers) and the small size of many CNCs, often this type of spectroscopy can reveal the structural contributions of amorphous or graphitic carbonaceous nanoscale segments into CNCs, based on the percentage of sp^2 - to sp^3 -carbon atoms. With the same aim, a technique that can be complementary to XPS is thermogravimetric analysis (TGA). Indeed, graphitized materials tend to decompose at higher temperatures and, therefore, the TGA profile provides a good indication of the graphitic or amorphous nature of the material at study. Additional information on the functional groups that are present in the structure of CNCs can be obtained using infrared (IR) and nuclear magnetic resonance (NMR) spectroscopies. In particular, ^1H and ^{13}C -NMR data are useful to verify the absence of the starting materials and small byproducts in the purified material. Further support for the absence of small molecular entities is offered by two-dimensional NMR spectroscopy, modeling, and optical spectroscopy, which give insights on the homogeneity of the CNC sample.¹¹

Chemists, physicists, materials scientists, mineralogists, and geoscientists too are interested in CNCs. This diversity of expertise, combined with the structural variability of CNCs, has been reflected in the terminology used to discuss the properties of CNCs and, in particular, their optical properties. To aid readers coming from different backgrounds, we briefly overview the types of an excited state that are most commonly encountered. To start with, the excited state of CNCs can be molecular-like, meaning that the excited state is localized onto a fragment having specific optically active structural features, as occurring in molecular fluorophores. Many amorphous CNCs display such excited states. In some other cases, the promotion of an electron to a higher-energy orbital creates a charge separation, described as an exciton, when the electron and hole are attracted by electrostatic forces. This is the typical description associated with semiconductor quantum dots (QDs) and is frequently used also to describe the excited state of CNCs, albeit inaccurate and incomplete. When the exciton is delocalized on the whole structure, the size of the structure dominates the energy of the associated transition, producing a quantum confinement effect. In CNCs, this gives some approximation to the observed optical phenomena, although unable to correctly describe the properties and origin

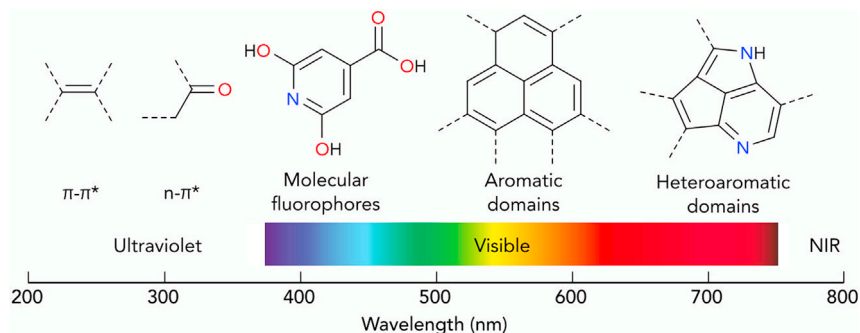


Figure 2. Functional units associated with light absorption

Representative structural units associated with light absorption across the UV-vis-NIR parts of the electromagnetic spectrum.

of many optical properties in CNCs. For example, the dependence of the emission wavelength on the excitation wavelength observed for most CNCs cannot be explained within this framework. Finally, in such complex materials, the so-called trap states can not only influence the observed behavior but be the goal of property engineering. The trapped states are typically associated with structural defects of the graphitic lattice or molecular-like states that interfere with the excited states responsible for the main optical transition. Again, this description being borrowed from the understanding of optical properties of semiconductors, cannot be, in fact, applicable here because the contribution of amorphous component is often substantially larger than that of the graphitic one.

As one can see, the description of the excited state is tightly associated with a structural knowledge and CNC representation as having a “core” and a “shell.” In CNCs, most often the term “shell” refers to the regions and functional groups of CNCs that are sensitive to the external environment. For QDs and CQDs, this may reflect a defined spatial separation of chemically distinct regions, but the correspondence is much less defined in the case of mostly amorphous systems like CNDs and CPDs. Therefore, the core-shell terminology has in many cases a rather different meaning compared to the one associated with QDs such as CdSe/ZnS QDs, where the core and shell have clearly defined phase boundary. This peculiarity of CNCs must be remembered when considering the description of excited-state properties in terms of core and shell.

LIGHT ABSORPTION

The simplest method to generate an excited state is the absorption of a photon. CNCs exhibit light absorption in the ultraviolet (UV) region with a long tail extending into the visible and near-infrared (NIR) regions.^{1,3} The energy structure, in particular, absorption characteristics of CNCs, are influenced by the size of π domains, shape, composition, and surface functional groups (Figure 2). The short wavelength bands below 300 nm correspond to $\pi \rightarrow \pi^*$ transition of sp^2 aromatic carbons, while the tail from 300 to 400 nm is due to the intrinsic absorption of $n \rightarrow \pi^*$ transition of C=O groups.¹² $n \rightarrow \pi^*$ and $\pi \rightarrow \pi^*$ charge transfers or interlayer charge transfer with a strong $\pi \rightarrow \pi^*$ component have also been associated with transitions in this spectral region.¹² The broad absorption bands above 400 nm may be attributed to extended aromatic domains or surface states, when sensitive to surface passivation or modification process. These modifications often affect the optical properties. In particular, red-shifted absorption can result from surface functional groups such as hydroxyl, carboxyl, and epoxy, which narrow the energy levels.¹² Moreover, a red-shift in

the absorption spectrum is commonly attained by introducing graphitic nitrogen into the carbon sp^2 lattice.¹³ Most CNCs display low absorption coefficients and a rather low emission quantum yields (QYs) in the NIR region. Therefore, developing strategies to improve light absorption and the NIR emission QY of CNCs remains an open challenge.

Two-photon absorption

NIR absorption is particularly desirable with respect to multi-photon optical processes, leading to the emission of light at a shorter wavelength than the excitation wavelength. Such property of CNCs is promising for numerous applications, such as biological imaging with enhanced tissue penetration and the reduced auto-fluorescence background offered by NIR excitation.¹⁴ Surface engineering of CNCs can lead to such two-photon or multi-photon processes. For instance, the surface interactions with sulfoxide or carbonyl groups in the outer layers and the edges produced NIR absorption bands and NIR emission. When excited at 1,400 nm, the surface oxidized CNCs can emit two-photon-induced NIR emission and three-photon-induced red emission.¹⁵ Polymers have also been used as passivating or functionalization agents to enhance the optoelectronic properties of CNCs. In particular, derivatives of polythiophene have been used for inducing sulfur doping in CNCs via the hydrothermal route, which exhibited efficient two-photon excitation, though, with a low QY of 0.2%.¹⁶ From these examples, it is clear that suitable interactions with the environment can facilitate multi-photon absorption, and among the different types of CNCs, nitrogen-doped CQDs (N-CQDs) appear as a promising platform to achieve multi-photon absorption. As an example, dopamine and *o*-phenylenediamine were used as precursors to prepare in a facile, high-output method NIR-emissive N-CQDs displaying two-photon fluorescence, which comes at a wavelength of 710 nm with a QY as high as 26.28%.¹⁷ From these examples, it emerges that heteroatom doping has a key role in promoting charge-transfer states responsible for two-photon absorption, preferentially in N-CQDs. Extending this strategy, co-doping of CNCs with N and F atoms promoted the formation of electron donor-acceptor interactions, allowing up to four-photon absorption.¹⁸

Absorption of circularly polarized light

As one kind of the chiral nanoparticles, CNCs represent an emerging type of chiral nanomaterials.^{19,20,21,22} Both their molecular structure and their three-dimensional nanoscale geometry give rise to a difference in light-matter interaction with left and right circularly polarized light. As one of the manifestations of these properties, CNCs display circular dichroism (CD), which implies different absorption coefficients for left-handed and right-handed circularly polarized light. The CD spectra give important structural information, e.g., about the identity of stereoisomers. Chiroptical properties are also essential for life sciences, medicine, analytical chemistry, photophysics, quantum phenomena, and telecommunications.²³

The first strategy to obtain chiral CNCs is the attachment of chiral moieties to the edges of graphene sheets (Figure 3A).^{24,22} For instance, functionalization of GQD by *L*- or *D*- cysteines afforded *L*-GQDs and *D*-GQDs, with mirror-symmetrical CD peak at 210–220 nm, corresponding to the molecular states of the amino acid groups, broadened by hybridization with edge groups of the graphene sheets.²² Furthermore, the resulting GQDs acquire a twisted mirror asymmetrical geometry and display a new mirror-symmetrical CD peak at 250–265 nm that is associated with the twisted nanoscale geometry of the graphene sheet, representing the delocalized (particle-wide) excitonic states.

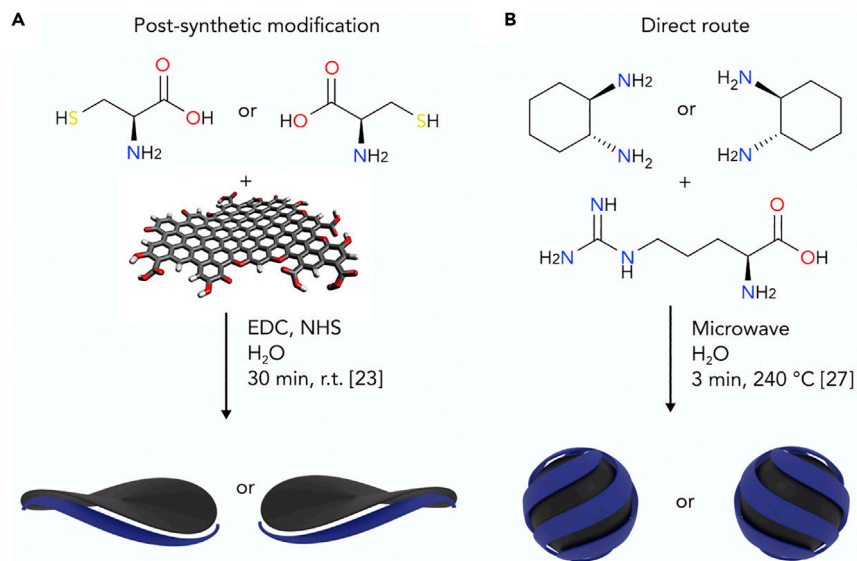


Figure 3. Strategies enabling circular dichroism

(A) Example of the post-synthetic route to impart chirality, by coupling the edge groups of achiral GQDs with enantiopure cysteines. EDC, 1-ethyl-3-(3-dimethylaminopropyl)carbodiimide; NHS, N-hydroxysuccinimide.

(B) Example of the direct route to chiral CNCs, obtained using chiral diamine precursors able to retain chirality under the employed synthetic conditions.

Chiral GQDs could be also synthesized by a simple esterification reaction of oxidized GQDs with enantiomerically pure (*R*)- or (*S*)-2-phenyl-1-propanol. These chiral GQDs were able to transfer the chirality to the supramolecular assemblies formed with small molecules such as pyrene.²⁵ Chiral CNCs were also obtained by surface passivation with chiral ligands, e.g., (–)-sparteine or (+)-sparteine.²⁶ Being suspended in water, these CNCs showed CD peaks at 195–220 nm, which can be attributed to the chiral molecular excited states of nanocolloids.

A different route to chiral CNCs is to introduce a chiral source during the synthesis of the nanomaterial. As an early example, chiral CNCs were prepared by hydrothermal treatment with citric acid and simultaneously capping with L- and D-cysteine to introduce chirality in the system.²⁷ Later on, chiral CNCs were synthesized from different chiral precursor molecules by incomplete carbonization of precursor molecules using D-methionine, D-glucose, D-glucosamine, and L-methionine (L-Met), L-aspartic acid, and L-alanine. A critical aspect of this strategy is that racemization often occurs under the harsh conditions necessary for the synthesis of CNCs. A system that showed a high tolerance to such conditions employed (*R,R*)- or (*S,S*)-1,2-cyclohexanediamine in combination with arginine, reacting in a microwave-assisted hydrothermal synthesis performed at 240°C to afford chiral CNCs (Figure 3B).^{21,28} The CD spectrum of (*R,R*)- or (*S,S*)-CNCs aqueous solution presents two negative or positive Cotton effects at 260 and 320 nm. These chiral CNCs were used to control the chirality of supramolecular porphyrin assemblies, showing that it is possible to use and transfer the chiral information embedded in CNCs for developing chiral composite materials and related applications.²¹ Chiral assemblies of CNCs or self-assembly of chiral nanocomposites/supraparticles may further advance the applications of chirality in catalysis, biology, and nanotechnology. In this regard, vortices have been utilized to induce chirality in graphene oxide (GO) aggregates.²⁹ These aggregates can in turn transfer chiral asymmetry to non-covalently bound porphyrin

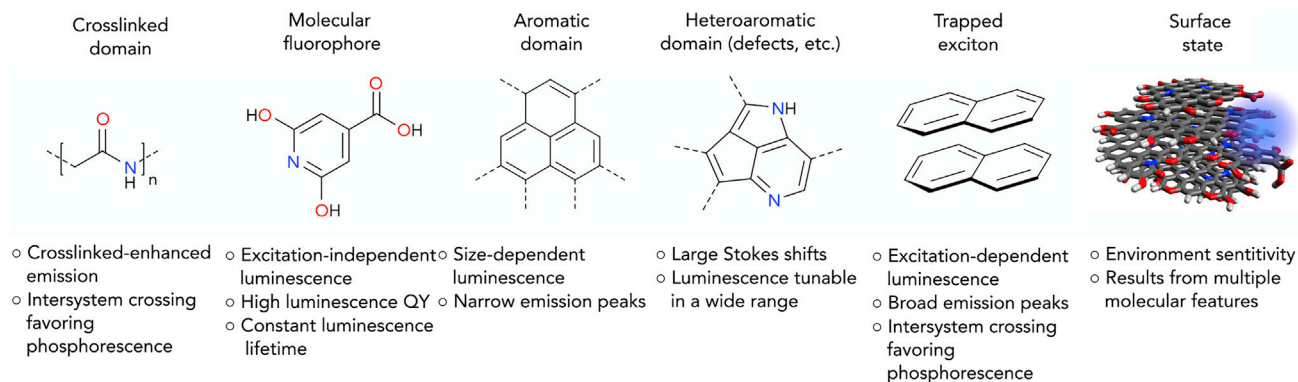


Figure 4. Types of fluorescent excited states encountered in CNCs

The stimulated light emission of CNCs can originate from each of the model structural features depicted, with distinctive emission properties listed below.

derivatives, inducing measurable CD signals. Stirred dispersions of GO could also be deposited on quartz to capture the transient, vortex-induced chirality of GO assemblies, providing an unusual route to composite materials that are unavailable by other means. Similarly, chiral composites from nanocarbons are made by macro-to-nano chirality transfer via twisting deformation that can serve as a unifying technological platform for chiral photonics in UV, vis, and NIR parts of the spectrum.³⁰ A facile and scalable method was recently developed to synthesize chiral photoluminescent N-doped CNCs on the surface of chiral cellulose nanocrystals.³¹ The geometrical arrangement of CNCs on the surface of twisted cellulose nanocrystals preserve the molecular chirality of the surface glucose, as confirmed by CD spectra, and allows fluorescence-detected CD, i.e., the observation of stronger emission upon excitation with circularly polarized light of one handedness, rather than the other, which should not be confused with circularly polarized emission.

FLUORESCENCE

An attractive feature of CNCs is their strong stimulated light emission, covering a wide spectral range and having moderate to high QYs. Several photoluminescence (PL) modes of CNCs may be highlighted: fluorescence, including delayed fluorescence, phosphorescence, and the aforementioned up-conversion PL.^{4–6} Among them, fluorescence emerges as the most common light-emitting process. Two factors that stimulated the investigation of CNC fluorescence are the frequent observation of large Stokes shifts and excitation-dependent emission spectra, which are uncommon features among molecular fluorophores and semiconductor nanoparticles. Therefore, much effort was invested into the determination of the emission origin, which remains one of the most debated aspects of CNCs. Approaching this question, it is important to remember the intrinsic variability of CNCs within the same sample, which could well be the source of the observed excitation-dependent emission spectra. Moreover, the energy structure and, hence, the mechanism of fluorescence is highly dependent on the synthetic routes and can vary largely across different categories of CNCs. Indeed, taking into account a wide variety of CNCs, several structural features responsible for fluorescence can be recognized (Figure 4): luminescent groups or fluorophores crosslinked within polymeric chains, sp^2 -conjugated domains, heteroatom luminescent centers within the carbon matrix, trapped excitons, and surface-related luminescent centers. It is worth mentioning that the CNCs can support multiple emissive centers, thus the origin of the emission can be a superposition of radiative recombination contributions from

their different types.³² Let us consider each possible origin of fluorescence in more detail.

Starting from the less carbonized types of CNCs, the emission originates from small units that are not usually associated with fluorescence and may become emissive when participating in a crosslinked network, due to vibrational restrictions or even electronic coupling.^{33,34} Crosslinking of sub-luminophores and fluorophores affects the optical transitions by promoting radiative transitions (increasing PL QY) and suppressing nonradiative transitions, which in addition to favoring the intersystem crossing activates the radiative transitions from triplet state (phosphorescence). This mechanism is often associated with blue emission color and is highly relevant for the widely used citric acid and ethylenediamine precursors, for which crosslinking can lead to blue fluorescence, together with the formation of citrazinic acid and its derivatives.^{35–37} In a seminal work, maleic acid and ethylenediamine were reacted hydrothermally affording CPDs with multicolor emission, in which the blue emission was attributed to fluorophore groups within polymer chains, while green and yellow emissions were attributed to the fluorophores formed by the interconnection of the polymeric chains.³⁸

At synthetic conditions related to the formation of CPDs and amorphous CNDs (Figure 1), the energy levels and emissive mechanism can be ascribed to the presence of fluorophores formed during the synthesis and linked or trapped into the polymeric network within CNCs.⁴ The presence of such molecule-like fluorophores is ubiquitous in the chemistry of bottom-up synthesized CNCs and requires thorough purification protocols.⁹ Emissive centers originating from molecular states possess excitation-independent emission with high QYs and PL lifetime remaining constant within the PL band.³⁹ While these emissive centers are linked to the surface of the CNCs, they can be easily photobleached and oxidized.

Another type of absorptive and emissive centers are sp^2 -conjugated domains, which can be also assigned as polycyclic aromatic hydrocarbon (PAH) domains and are likely responsible for luminescence in the visible region. Weak size-dependent luminescence is observed for less carbonized and amorphous CNCs, where sp^2 domains are connected via an amorphous carbon network. In this context, it was shown that the CNDs optical spectra coincide with that of a matrix-embedded mixture of small PAHs, such as pyrene, perylene, and anthracene.⁴⁰ Importantly, as it was shown for the proposed “cocktail of PAHs,” the formation of excimers or exciplexes, i.e., exciton trapping, gives rise to Stokes shifts comparable to those observed for CNCs. In the case of CNCs, different types of emissive units play the role of PAHs resulting in the broad and excitation-dependent emission peak position and radiative lifetimes with a gradual decrease in its intensity. Only at a high carbonization degree, the position of the luminescence peak may be associated with the size of CNCs. Indeed, strong size dependence is more easily observed for highly carbonized nanocolloids (CQDs and GQDs), where quantum confinement of the excitons can be realized.^{41,42} Recently, triangular sp^2 -domain CNCs were synthesized from phloroglucinol via dehydration and carbonization processes.⁴¹ These CNCs possess a pronounced size-dependent luminescence and high QYs, up to 72%, accompanied by extremely narrow emission, having a full width at half maximum (FWHM) of less than 30 nm.

Opportunities for engineering the emissive transitions in CNCs expand upon doping of the CNCs via synthesis with precursors containing elements such as nitrogen, boron, sulfur, phosphorus, or metal ions. In highly carbonized structures, the dopant atoms are integrated into the aromatic rings, perturbing the sp^2 domain lattice, which in turn leads to additional energy levels. One example regards the use of

N-rich precursors such as 2,3-phenazinediamine with citric acid, leading to a 188 nm Stokes shift and a QY of 24%.⁴³ Moreover, the use of bare folic acid, including an N-rich aromatic network, with amine, hydroxyl, and carboxylic groups, resulted in CNCs with QYs as high as 94.5%.⁴⁴ The presence of heteroatoms can also create defect states in the aromatic domains, leading to localized emissive (or dark) states.

In many cases, the emission is also dependent on the CNC surface. In the case of GQD, the carbon network morphology, i.e., armchair and zigzag edges affect the emission properties.⁴² For all types of CNCs, chemical modification of the surface can affect the luminescence properties. Indeed, as a recurrent strategy, luminescence can be tuned via oxidation or introducing functional groups such as amines or thiols. Frequently, covalent bonding affects the energy structure of π -conjugated system.⁴⁵ Indeed, the electron-donating or withdrawing nature of the introduced functional group such as amine or carboxyl group can shift the highest occupied molecular orbital (HOMO) energy level (increase or decrease it, respectively). Also, it was shown that surface passivation and functionalization increase the PL QY.⁴⁶ Finally, when surface states are involved, the chemical environment can modulate the optical properties: emission band positions and QYs are highly sensitive to the pH of the environment and the chemical properties of the solvents. In most cases, the highest QY is observed for increased pH values (starting from pH = 5). Oxygen-containing groups of the solvent can interact with amine groups at the surface of CNCs, which results in the increased absorption in the NIR region and enhancement of the related PL QY.¹⁵ The optical transitions of CNCs can be also affected by environmental polarity and the coordinative nature of the solvent, as was seen in CNCs that were intrinsically doped with Mn(II)⁴⁷ where metal-to-ligand charge-transfer (MLCT) absorptions occurred. Thus, in non-polar media, fluorophore emission dominates, while in polar environments, energy transfer to the MLCT state is downhill and MLCT emission governs. Additionally, the parameters of the solvents such as polarity and protic/aprotic nature can impact the CNCs emission via solvent relaxation process and solvent-induced aggregation of CNCs.

Despite intense investigation, the fluorescent properties of CNCs still offer room for improvement. Obtaining CNCs that fluoresce in the red region with a high QY remains challenging.⁴⁸ Promising results have been developed taking advantage of the oxidative polymerization of aromatic units, such as phenylenediamine or including formamide in citric-acid-based hydrothermal synthesis.^{48–50} Yet, to achieve high QY emission in the far red and NIR region, additional efforts are demanded.

Spectroscopic insights into light emission processes

In almost all CNCs, the synergistic effect of doping, increasing the sp^2 -domain size, and functionalization of CNC surface is most likely taking place. Unfortunately, it is quite often difficult to change a single synthetic parameter and identify its individual influence on the energy level structure, because the mutual influence of different parameters is often unintelligible. Therefore, to gain insights into the electronic structure of CNCs and its excited-state behavior, it is necessary to carry out a general analysis. Such analysis includes the study of morphology and chemical composition, along with a thorough analysis of CNC optical responses, traditionally based on optical spectroscopies, in particular optical absorption and PL. Since, in most cases, the typical luminescence band of CNCs is non-structured and lies in the blue spectral region, more advanced experimental techniques are in demand to disclose the excited-state levels of CNCs and investigate the processes following photoexcitation (Figure 5).

Through time-resolved absorption spectroscopy, the fast relaxation processes following excitation are revealed, which helps to understand the architecture of



Technique	Insight
Transient absorption and Time-correlated single photon counting	⊥ Excited state type and lifetime
Fluorescence anisotropy	↻ Rotational freedom
Fluorescence correlation spectroscopy	• → Diffusion coefficient (size)
Single molecule experiments	••• Individual vs bulk comparison

Figure 5. Spectroscopic techniques giving additional insights on luminescence

Experimental techniques that can be employed to analyze excited-state properties of CNCs, with a focus on fluorescent states. The main insights offered by each technique are indicated on the right.

CNC excited states. Importantly, the transient absorption spectra allow to distinguish dark states, together with the bright ones. This capability was exemplified by early work, which ascribed the luminescence of QDs to molecular-like states, while identifying also a dark quantum-confined state originating from the intrinsic band gap of GO, which was retained in QDs.⁵¹ Using the same experimental setup, it is possible to observe time-resolved photoluminescence. Observing the evolution of the luminescence spectrum in time allows to resolve its components. This operation is particularly useful in the study of CNCs, which often display multiple emissive states. Indeed, thanks to time-resolved PL, it became possible to distinguish several emission states within multiemissive CNCs and explain their behavior. Most of the information that can be obtained from the analysis of time-resolved PL can also be obtained using time-correlated single-photon counting (TCSPC), which is the preferred technique to measure the lifetime of an emissive state. A big advantage of TCSPC over transient absorption and time-resolved emission is the simplicity of the associated experimental setup, which does not require delicate and time-consuming optics alignment, thus it is associated with fast experiments. Therefore, TCSPC experiments give rapid access to the lifetime of the excited state, which is a critical parameter, because it dictates the time available to the excited state to engage in energy and electron transfer processes or other quenching phenomena.

A set of measurements that can be closely associated with TCSPC from an experimental perspective are those associated with anisotropy. Practically, these require the use of polarizers, in combination with standard emission setups. Anisotropy measurements are a helpful tool in understanding the origin of the excited states in CNCs, because they relate the symmetry and mutual arrangement between absorption and emission dipoles. In addition, time-resolved anisotropy reveals the timescale on which anisotropy is lost. This process is most often associated with energy migration or rotation of the fluorophore. Therefore, anisotropy can reveal its interaction/interconnection with the environment and may offer insights on the size and shape of the CNC luminescent centers. Implementing this approach, it was proposed that the fluorescence center of a CNC synthesized from citric acid and ethanolamine, with a size of 8.3 nm, is embedded in a non-rigid medium, because it is free to rotate, as inferred from the fast depolarization observed.⁵²

A complementary technique is fluorescence correlation spectroscopy (FCS), which investigates the correlation of luminescence within a focal volume. From these data, one can estimate the diffusion coefficient of the luminescent center, thus inferring its size, shape, and the local environment. With minimal adaptation, rotational freedom can also be deduced. FCS measurements have suggested that in some

CNCs the luminescent center has a size up to 1 nm, which corresponds to that of small organic dyes.^{53,54} Importantly, excitation at different wavelengths afforded different diffusion coefficients. Taken together, these measurements support an intrinsic diversity for CPDs and CNDs compared to more carbonized CNCs, due to the presence of small molecular fluorophores. More detailed information was accessed via the time-resolved electron paramagnetic resonance (EPR) technique (*vide infra*), leading to the same conclusion.

Single-particle spectroscopy insights

Some of the most fascinating investigations involving CNCs are those implementing single-particle spectroscopy, a development that is important not only for revealing the origin of CNCs emission but also for sensing and bio-labeling applications.⁵⁵ The most immediate question that can be answered is whether the excitation-dependent emission observed in bulk experiments originates from the intrinsic diversity of CNC samples or it is intrinsic of single CNCs. In a seminal work, it was shown that the bulk emission spectrum is the average signal of the spectra from the individual CNCs, having excitation-independent emission at the single-particle level, exhibiting narrow FWHM and mono-exponential luminescence decay.⁵⁶ Moreover, the authors claimed that the CNC emission originates from the recombination of photogenerated charges on defect centers involving a strong coupling between the electronic transition and collective vibrations of the lattice structure. Recently, a single-molecule study relying on single-molecule absorption detected by scanning-tunneling microscopy, allowed to image electronic states at the sub-particle level, demonstrating that both localized (defect) and diffused electronic states can be present.⁵⁷ As in the aforementioned single-particle study, the emission was attributed to defect states, pointing at surface oxidation as a strategy to obtain low-energy emission, in line with bulk experiments.⁵⁸ Significantly, the study employed CNCs obtained from 1,2,4,5-benzenetetracarboxylic acid and 2,7-diaminofluorene, obtaining CNCs that were separated by column chromatography over a few days. By doing this, CNCs of similar sizes were separated according to their polarity, leading to apparently homogeneous behavior at the single-particle level. Taken together, these observations point to the importance of chemical functionalities determining the molecular states and optical properties of CNCs.

When discussing the single-particle measurements, one of their main characteristics is "blinking," which can significantly affect the future applications of CNCs. In general, blinking involves the switching of a single emitter between "on" and "off" states and is described by frequency, duty cycle, and intensity. Depending on the applications, different requirements are set for these parameters. For instance, to trace analytes in biological systems *in vivo*, the high emission intensity of a single particle along with the long duration of the «on» state is required. On the contrary, for high spatial resolution, single particles possessing a high intensity and low duty cycle are in demand. Despite initial reports suggesting a non-blinking nature of CNCs, intrinsic fluorescent fluctuations of CNCs have been reported and this behavior seems prevalent.⁵⁹ This behavior suggests the presence of different energy traps and various surface oxidation states within the CNC energy structure. At the same time, CNCs possess desirable parameters for luminescent imaging at the single-particle level. As an example, they display higher photon output compared to that of organic dyes, which has been reported, as well as low «on» duty cycle (around 10^{-3}) compared to semiconductor nanoparticles.⁶⁰ Recent reports also showed that the blinking parameters are highly dependent on the chemical environment of the CNCs, such as the presence of electron donor or acceptor molecules. This behavior expands the opportunities for sensing applications on a single-particle level. All



Figure 6. Strategies promoting phosphorescence of CNCs

Selected methods of structural control over phosphorescence from CNCs or long-lasting fluorescence due to thermally activated delayed fluorescence.

these findings suggest that the CNCs are suitable and prospective emissive nanoparticles for future bio-imaging applications.

PHOSPHORESCENCE AND TRIPLET STATES

Contrary to fluorescence, the studies on phosphorescence in CNCs are infrequent. Phosphorescence, sometimes referred to as afterglow luminescence, involves a radiative transition between states having a different multiplicity. In organic systems, it typically requires the intersystem crossing from the excited singlet state to an excited triplet state, which is spin-forbidden in classical systems. Heavy atoms facilitate intersystem crossing due to strong spin-orbit coupling with singlet excited state. Transitions between states of different symmetry are also favored. For example, when $n-\pi^*$ states are present, intersystem crossing to $\pi-\pi^*$ states becomes possible. For this reason, although the population of triplet states in aromatic hydrocarbons is not favored, the same process becomes favored in aromatic N-heterocycles and carbonyl compounds.⁶¹ Therefore, in CNCs, doping by heteroatoms such as nitrogen favors the intersystem crossing, as a result of the additional $n-\pi^*$ states having a relatively small gap between singlet and triplet states. Thus, the population of triplet states seems a likely process in CNCs.

Triplet states may deactivate radiatively, giving off phosphorescence. However, triplet states may also be non-luminescent as deactivation can easily occur, via molecular vibrations. The understanding of CNCs energy structure, together with the development of suitable synthetic routes, suggests that to promote phosphorescence, the molecular groups responsible for this process should be immobilized, thus suppressing vibrational and rotational motions. Shielding from molecular oxygen should also prevent deactivation via energy transfer to oxygen. In line with these expectations, phosphorescence has been observed for CNCs embedded in the rigid matrices (Figure 6).⁶² Several inorganic and polymeric matrices proved to be effective, including silica gel, layered double hydroxides, zeolites, molecular crystals, polyvinyl alcohol (PVA), and polyurethane. Chemical modifications affording to crosslinking were also employed successfully and simple operations, such as freezing, drying to the powder, or drop-casting to paper, could also favor phosphorescence in some cases. When the phosphorescent centers in CNCs are self-protected and self-immobilized, room temperature phosphorescence becomes possible even for bare CNCs dispersions or solids.⁶³ These desirable features seem more frequently observed in CPDs, which are indeed particularly promising in this context.^{64,65} As an example, the longest lifetime of 1.46 s at 525 nm was measured for the powder of CPDs with a size of 3.4 nm obtained from ethanolamine and phosphoric acid.⁶⁶ Similarly, the highest solid-state luminescence QY reported so far (41%) pertains to white-light-emitting CPDs, which showed prolonged stability under UV irradiation and a luminous efficacy comparable to that of rare-earth phosphors.⁶⁷ Yet, substantial efforts are still required to engineer bare CNCs that are phosphorescent in simple water solutions.⁶²

Light emission with long lifetimes can also be achieved via thermally activated delayed fluorescence. In this case, a long-lived dark triplet state is thermally equilibrated with an emissive singlet state that serves as the main radiative deactivation pathway. This effect was observed for CNCs bonded to SiO₂ particles, in which a contribution of phosphorescence was also present.⁶⁸ This is a tangible example that dark triplet states can be non-innocent. Indeed, the intersystem crossing is most likely a ubiquitous process in CNCs, which goes frequently unnoticed, but could be potentially exploited. An elegant study in which the formation of dark triplet states was proven, exploited time-resolved EPR spectroscopy.⁵³ Singlet states are diamagnetic and EPR-inactive, whereas triplet states can be detected by EPR. CNCs synthesized from citric acid and ethylenediamine, or arginine and ethylenediamine, were studied, and it was found that triplet states with a lifetime of about 20 μs are generated upon photoexcitation. The features of the obtained EPR spectrum were compatible with a triplet state localized on aromatic domains composed of three to five aromatic rings. Coherently, with the studies focusing on fluorescence, different domains were populated depending on the excitation wavelength, suggesting an intrinsic heterogeneity of the sample. Similar findings were reported also for CNCs obtained from the hydrothermal treatment of phenylenediamines.⁵⁴

PHOTON- AND CHARGE-MANAGEMENT

Once in the excited state, CNCs are susceptible to energy and electron transfer processes. On one hand, energy transfer is, next to light absorption, *vide supra*, one of the most fundamental processes in terms of photon-management. It is often associated with the need for light-harvesting. Electron transfer, on the other hand, is the key process in charge management and is the basis for most light-driven technological applications. Given the modest ability of CNCs to absorb light, energy transfer processes received limited attention. Nonetheless, CNCs offer pathways to materials with photon-management capabilities arising from energy transfer processes. These are engineered by, for example, tuning plasmonic couplings with metallic nanostructures or to act as sensors. In stark contrast, charge-transfer effects have been investigated in great detail. It was shown that CNCs serve as either electron donors or acceptors in several cases. They even engage as an innocent platform for enabling interchromophoric interactions. The ultimate goal is to optimize photon- and charge-management in the design of photocatalytic systems that allow transforming light into fuels.

When introducing photoinduced processes that are associated with CNCs, it should be mentioned that the elephant in the room is structural features, and, in particular, those associated with surface interactions. They are often overlooked, but they have the utmost importance in modulating energy and electron transfer interactions (Figure 7). Furthermore, they can lead to the spontaneous organization of CNCs into more complex structures capable of directional charge or photon transports.¹¹ The interactions employed so far encompass the most common interactions. Yet, they are mostly based on simple carboxylic and amino groups, which are commonly formed throughout the CNC synthesis. This suggests that there is ample room for improving the properties of CNCs. Moreover, in the overwhelming majority of cases—if not all—the information on the surface groups is limited and approximate, due to the highly challenging nature of CNCs from a structural perspective. Because of the tight relation of structural features with optical processes, this central issue hampers the optimal engineering for photon- and charge management.

Photon-management: plasmonic coupling

Plasmonic coupling is freely tunable thanks to the ability of CNCs to engage in energy transfer phenomena with metallic nanostructures. The geometrical and

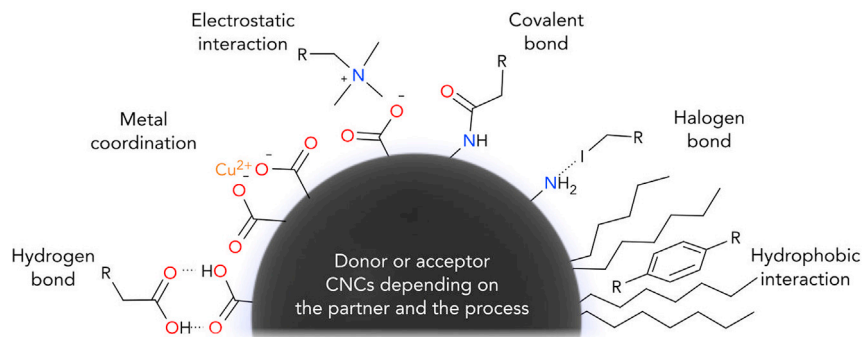


Figure 7. Surface interactions involved in photoinduced processes

Overview of the supramolecular and covalent interactions that have been exploited in systems in which photoinduced energy and electron transfer take place.

chemical properties of those metallic nanostructures, exert a strong impact on energy transfer interaction. These have been investigated with a focus on photon-management. In particular, a hybrid material consisting of a plasmonic silver hole array, with a hole diameter of 160 nm, embedded on top with CNCs dispersed in a thin PVA film, shows the efficient coupling between donor CNCs states and acceptor plasmonic modes (Figure 8).⁶⁹ The functional groups of the CD surfaces induce dipoles on the silver surface, modifying the work function, thus the absorption and emission properties. This effect is modulated by means of using different CNCs, thus tuning the optical responses. In the case of CNCs, which bear electron-donating amino groups, the emission is detected at 550 nm, whereas electron-withdrawing ester groups shift the emission to about 580 nm. Additionally, it has been demonstrated that the energy transfer efficiency is controlled by changing the silver hole array periodicity, which allows tuning the surface plasmon modes to be in resonance or off-resonance to CNC states.

Photon-management: sensing

Photon-management in CNCs has been widely exploited for sensing purposes, relying on energy transfer processes between CNCs and different acceptors. The interested reader is directed to specialized reviews.⁷⁰ Here, we describe, in more detail, two exemplificative cases, to highlight the versatility of CNCs in this area. In the first case, rhodamine 6G moieties were covalently immobilized onto CNCs, affording a hybrid that operates as a turn-off Al^{3+} sensor (Figure 9A).⁷¹ Exposure to Al^{3+} induces a ring-opening reaction at the rhodamine, which results in a better spectral overlap between CNC emission and rhodamine absorption. This process favors energy transfer from the CNC to rhodamine, causing an increase in emission intensity at long wavelengths. To illustrate the versatility of CNCs as sensors based on energy transfer, the second example of choice relies on supramolecular interactions affording a turn-on sensor (Figure 9B). In particular, fluorescein amidite-labeled single-stranded DNA (ssDNA) adsorbs onto CNCs, likely via electrostatic interactions, enabling an energy transfer from the CNCs to the luminescent ssDNA, which quenches the CNC emission.⁷² However, the emission is reinstated upon the addition of complementary micro RNA-9-1 (miRNA-9-1) gene, which is associated with several diseases, including breast cancer.

Charge-management: tuning the directionality of charge transfer

CNCs are highly versatile in terms of charge management and the directionality of charge transfer has been tuned with great success. CNCs, for example, have been combined in a non-covalent fashion with molecular electron donors and acceptors.

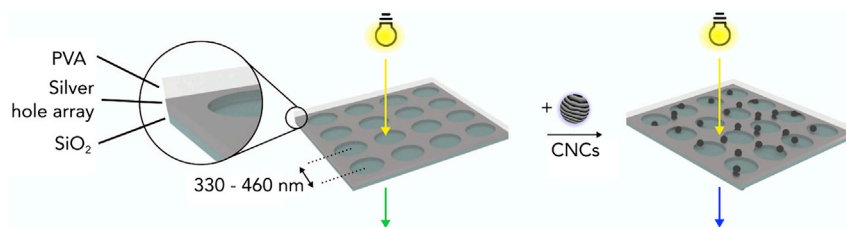


Figure 8. Plasmonic coupling with nanostructured materials

When CNCs are dispersed on a silver hole array, their electronic interaction with plasmonic modes tunes the optical response of the nanomaterial, affecting both the transmittance and the emission properties.

The resulting assemblies showed photoinduced electron transfer activity, which is modulated by supramolecular interactions. Hereby, the emission of the negatively charged CNCs is quenched upon the addition of triethanolamine (TEOA), which transfers electrons to photoexcited CNCs. Quenching of the CNC luminescence is observed also upon the addition of methylviologen (MV^{2+}), a common electron acceptor (Figure 10).⁷³ In particular, Stern-Volmer quenching constants and binding constants for the CNC/ MV^{2+} pair are two orders of magnitude larger than those for CNC/TEOA. This evidence indicates that photoinduced electron transfer with MV^{2+} is more efficient due to electrostatic interactions between negatively charged CNCs and positively charged MV^{2+} . Nevertheless, the transient products of electron transfer, i.e., reduced MV^{2+} , and oxidized TEOA, were detected using ultrafast transient absorption experiments in both cases. However, further rationalization of the photoinduced catalytic reduction of MV^{2+} , which represents a widespread model system, was found to be difficult, indicating that the catalytic activity is regulated by a complex interplay between several factors.⁷⁴

Charge-management: symmetry-breaking charge transfer

Notably, CNCs have been employed as a spectator rather than as an active electron donor or acceptor. They serve as a scaffold, which supports interactions between chromophores bound to their surface. In CND-ZnPc conjugates, strong ground state interactions lead to the splitting of the ZnPc Q-band absorption, also known as Davydov splitting. Upon ZnPc excitation and subsequent excited-state dynamics, a pair of interacting ZnPcs undergo simultaneous oxidation and reduction to afford a charge-separated state, which is symmetry broken.^{75,76} Nevertheless, the effects that come into play in these hybrids can be difficult to control, ultimately because the chemical structures of CNCs, thus the functionalization anchors, are not clearly defined. This complexity can be appreciated by comparing CND-ZnPc with covalent hybrids of CNDs with a tetraaryl porphyrin (TArP) (Figure 11), where a different situation is observed. In the case of CND-TArP, in the ground state, the two components exhibit minimal interactions, while excitation leads to an electron transfer from the porphyrin to the CND. However, the precise tailoring of the excited-state dynamics is closely linked with the ability of disclosing or tuning structural features, which, at present, remain largely unpredictable. To date, in most cases, interchromophore interaction is not observed.

Charge-management: gating charge transfer

Charge-management has evolved in CNCs up to a point that it is possible to gate charge transfer processes exploiting surface interactions. A drastic effect is observed when comparing electron transfer between negatively charged CNCs and positively or negatively charged electron acceptors. Perylendiimides (PDIs)

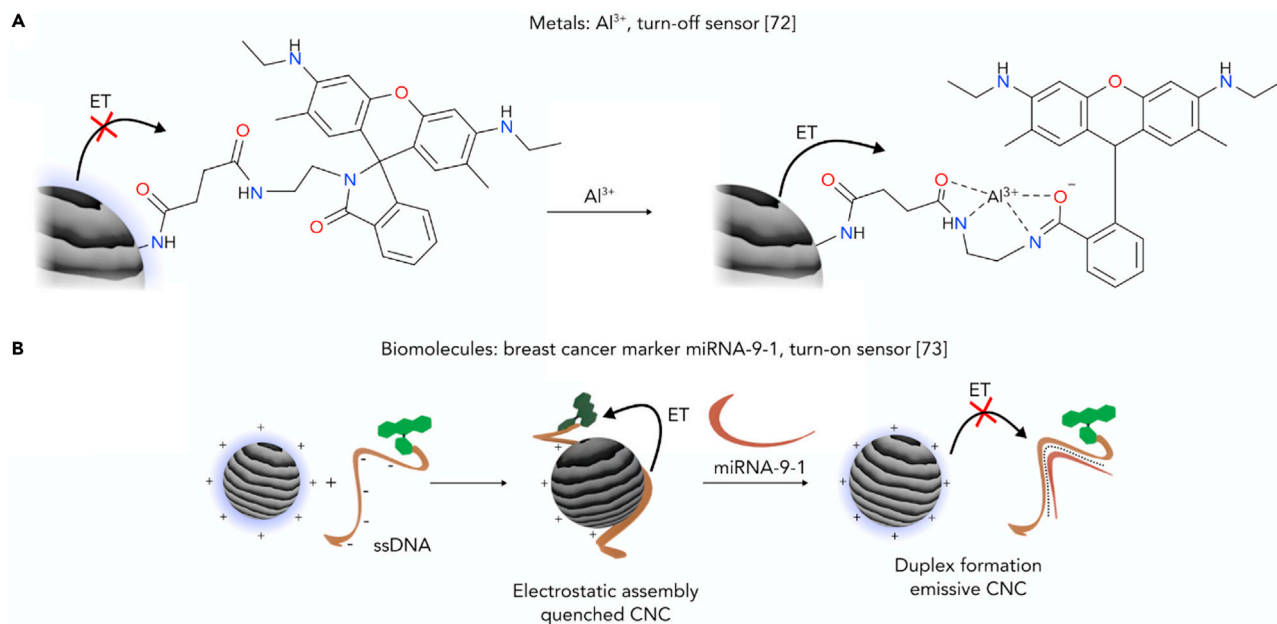


Figure 9. Energy transfer for sensing applications

(A) Turn-off sensor for the detection of Al^{3+} , which induces a ring-opening reaction at a covalently bound rhodamine 6G moiety. (B) Turn-on sensor for the detection of miRNA-9-1, based on the interplay of supramolecular electrostatic and hydrogen bonding interactions between CNCs and nucleic acids. ET, energy transfer.

carrying at their imide positions ammonium groups, on one hand, and carboxylate residues, on the other hand, led respectively to positively and negatively charged PDIs. Only ammonium-PDIs efficiently act as a photoinduced electron acceptor together with CNCs and the ammonium-PDI radical anion signature is easily detected by transient absorption on the picosecond timescale (Figure 12).⁷⁷ Indeed, when carboxylate-PDI is employed, neither emission quenching nor radical anion fingerprints are observed, indicating that electrostatic repulsions completely hinder photoinduced electron transfer. Opposite electrostatic interactions were also exploited in CNC/Ni-phthalocyanine mixtures, in which negatively charged Ni-phthalocyanine quenches the emission of positively charged CNCs.⁷⁸

Photon- and charge-management: photocatalysis

Ultimately, the conversion of solar light into chemical fuels requires a precise combination of photon- and charge-management at the molecular level, that is, a precise control of energy and charge transfer processes. To this end, photocatalytic model systems containing CNCs are being developed. There, the energy of the absorbed photons is funneled to a reaction center where charge separation and reactivity take place. Several examples are covered below to illustrate that, in the search for metal-free photoredox catalysts, CNCs offer a versatile, inexpensive, and safe platform.⁷⁹ These properties are ideal for technological applications and make it desirable to expand the catalytic capabilities of CNCs.

In this context, CNCs without any modification or co-catalyst were able to photocatalyze the hydrogen generation reaction from water under UV light.⁸⁰ To shift the photocatalytic activity to the visible, eosin Y was used as a sensitizer.⁸¹ In a related contribution, it was shown that there is a trade-off between the emission QY and the photocatalytic activity toward hydrogen generation from water.⁸² When the preparation procedure

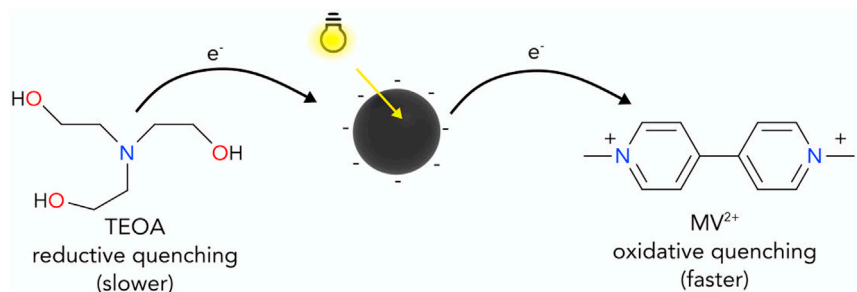


Figure 10. Oxidative or reductive photoinduced charge transfer

Both TEOA and MV^{2+} can quench CNCs excited state, however, for negatively charged CNCs, the oxidative quenching is faster.

involves moderate quantities of nitrogen, the N-content of the CNCs is mainly related to graphitic N-atoms and results in high emission QYs. In contrast, if either very high or very low nitrogen-to-carbon ratios were to be used in the syntheses, the majority of N-atoms would be placed at the edges of the aromatic domains. Peripheral N-sites promote trapping photogenerated electrons, facilitating charge separation, and enhancing photocatalytic hydrogen generation.

In a biomimetic sense, a particularly powerful strategy to expand the photoredox capabilities of CNCs is to interface them with redox enzymes. In this regard, surface engineering of CNCs proved essential, to establish favorable electrostatic interactions with redox enzymes. In a prominent example, positively charged, ammonium-terminated CNCs transfer electrons to negatively charged fumarate reductase (FccA), which reduces fumarate to succinate, and a hydrogenase (H_2ase).⁸³ Proof of the critical role of electrostatic interactions was provided by control experiments performed using carboxylate-terminated CNCs, which display little or no activity. Adding to the complexity in photon- and charge management, it was demonstrated that biocatalysis could be mediated by organometallic complexes. Indeed, CNCs were found to efficiently photo-reduce an organometallic electron mediator, which subsequently reduced synthetic nicotinamide cofactor analogs ($sNAD^+$), leading to asymmetric hydrogenation of double bonds catalyzed by the reductase old yellow enzyme (Figure 13A).⁸⁴ Besides biocatalytic approaches, bare amine-rich CNCs obtained from arginine and ethylenediamine were shown to catalyze perfluoroalkylation reactions (Figure 13B).⁸⁵ The proposed mechanism involves a halogen bond interaction that brings the iodoperfluoroalkyl substrate in proximity to CNCs, thus facilitating an electron transfer process from the CNC to the substrate, initiating a radical chain reaction.

System optimization is a critical tool in the area of photon- and charge management. This becomes clear when considering CNCs, which were combined with a molecular $\{Ni(diphosphine)_2\}$ hydrogen evolution catalyst. By means of a photoinduced electron and hole transfer involving CNCs, the reducing equivalents engage in hydrogen production upon solar irradiation (Figure 13C).⁸⁶ The system operates in water at pH 6, involves EDTA as a sacrificial electron donor, and is limited by the catalyst lifetime that causes hydrogen evolution to be negligible after 6 h. However, the use of tris(carboxyethyl)phosphine/ascorbic acid as a sacrificial electron donor avoids the formation of oxidation intermediates or products that inactivate the catalyst. This extends the Ni catalyst lifetime of five times. Catalytic activity is further increased when amorphous CNCs are graphitized and the core is N-doped.⁸⁷ The influence of each structural core modification was separately addressed. On one hand, core graphitization enhances CNC light absorption. On the other hand, N-

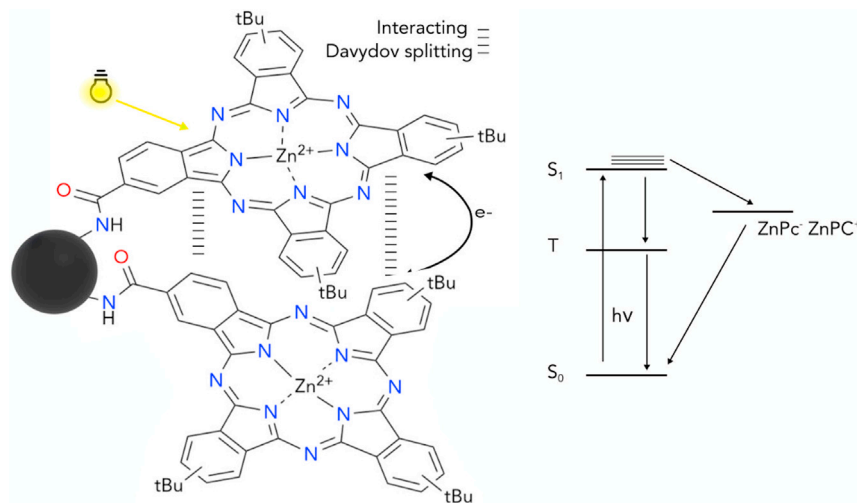


Figure 11. Symmetry-breaking charge transfer

Schematic representation and Jablonski diagram of a covalent CNC-ZnPC hybrid.

doping promotes the photogeneration of reactive electrons via hole scavenging by EDTA. Thus, reduced CNCs engage in an electron transfer process to the catalyst, which results in efficient hydrogen generation.

As a complement to hydrogen production, oxygen evolution has also been realized with CNCs. This documents, uniquely, the control over photon- and charge management, owing to the fact that charge directionality in oxygen evolution is opposite from that needed for hydrogen evolution. As a leading example, we wish to refer to self-assembled hybrids consisting of CNCs and cobalt polyoxometalate (Co-POM), which were studied using persulfate, as the sacrificial electron acceptor.⁸⁸ Upon visible light excitation, photoinduced hole transfer from CNCs to Co-POM results in a superior oxygen production, in comparison with the results obtained upon replacement of CNCs by $[\text{Ru}(\text{bpy})_3]^{2+}$ (bpy = 2,2'-bipyridine). Furthermore, in a CNC/ $\text{Co}_3\text{O}_4/\text{Fe}_2\text{O}_3$ composite, synergistic effects between CNCs and Co_3O_4 promote the photoelectrochemical water oxidation activity on Fe_2O_3 photoanodes via a two-step-two-electron pathway.⁸⁹ In this system, CNCs oxidize H_2O_2 to O_2 and, in addition, accelerate the slow oxidation of H_2O to H_2O_2 via Co_3O_4 , enhancing the photocurrent density in comparison with the bare photoanode and the $\text{Co}_3\text{O}_4/\text{Fe}_2\text{O}_3$ photoanode. Finally, both redox reactions involved in water splitting are catalyzed by a CNC/ BiVO_4 composite, where CNCs and BiVO_4 nanoparticles provide the reduction and oxidation active sites, respectively, in the absence of any sacrificial agents.⁹⁰ Overall, a hydrogen evolution rate over four times higher than just BiVO_4 nanoparticles is determined and stoichiometric amounts of H_2 and O_2 (1.8:1) are produced, in contrast to the non-stoichiometric production (0.06:1) detected for BiVO_4 nanoparticles alone.

CONCLUSIONS AND OUTLOOK

As occurred in other fields, the rapid development of CNCs resembled a gold rush.⁹¹ After more than 15 years from their discovery, it is safe to state that CNCs have demonstrated their potential, but time has come to reflect on the fundamental features of this relatively young material, to enable further progress. The emission properties of CNCs have sparked much interest, in particular regarding the origin of their typical excitation-dependent emission spectrum. Attempts have been made to reconcile all the available evidence under the framework of a prevalent emission mechanism. However, CNCs

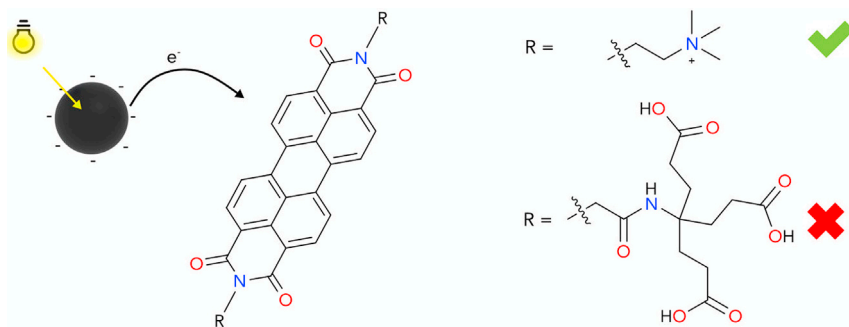


Figure 12. Photoinduced charge transfer facilitated by supramolecular interactions

Perylene bisimide reduction is an example of the photoinduced process enabled by complementary electrostatic interactions.

have an inherent variability, even within the same sample, that demands to embrace complexity, rather than forcing seemingly contrasting pieces of evidence under a single framework. For the same reason, experimental observations should be critically dissected and questions arise on the validity of rationalizations that merge information obtained on different types of CNCs. This consideration remains true even in many cases in which a single parameter is changed, since many different aspects of CNCs are tightly, yet obscurely, interconnected. Thus, when discussing the optical properties of CNCs, structural features emerge as the elephant in the room, since the correct attribution of optical processes to the responsible structural feature is essential. In a striking example, separation based on polarity revealed significantly different populations of CNCs, which would have been analyzed together using the most classical separation techniques that operate by size.⁵⁷ On top of this, many of the discussed examples on energy and electron transfer highlighted the role of surface interactions as key in regulating the observed behavior. Therefore, for the fundamental understanding of CNCs, it seems reasonable to focus on consolidated architectures and deepen the available knowledge. One may imagine that in the future, advances in electron microscopies may allow to determine the structure of CNCs. Addressing and engineering structural aspects of CNCs, including their chiral asymmetries, will unlock further developments associated with the optical properties of CNCs. In this process, the central question will shift from if a certain process is possible to how CNCs should be optimally engineered to perform a certain task. Yet, all the aspects covered in this review offer significant room for improvement. Shifting and enhancing the absorbance into the red and NIR region, achieving circularly polarized luminescence, facilitating phosphorescence in solution, engineering delicate excited-state processes such as singlet fission, or supporting multi-electron processes at the CNCs represent some of these opportunities. Importantly, advancements will also rely on engineering cascades of synergistic excited-state processes in functional hybrid nanomaterials. Utilization of chiral CNCs in enantioselective (photo)catalysis can also be expected.⁹² The biocompatibility and Earth-friendliness of CNC represent a marked advantage over semiconductor nanoparticles used in the past for chiral catalysis.⁹³ Finally, engineering optical properties in CNCs processable in aqueous and organic solvents will considerably expand the opportunities for the technological application of CNCs. At this crossroad between chemistry, material science, and photophysics, the future of CNCs looks bright.

ACKNOWLEDGMENTS

M. Prato is the AXA Chair for Carbon Bionanotechnology (2016–2023). This work was supported by the University of Trieste, INSTM; the Italian Ministry of Education MIUR (cofin Prot. 2017PBXPN4); the Spanish Ministry of Science, Innovation and

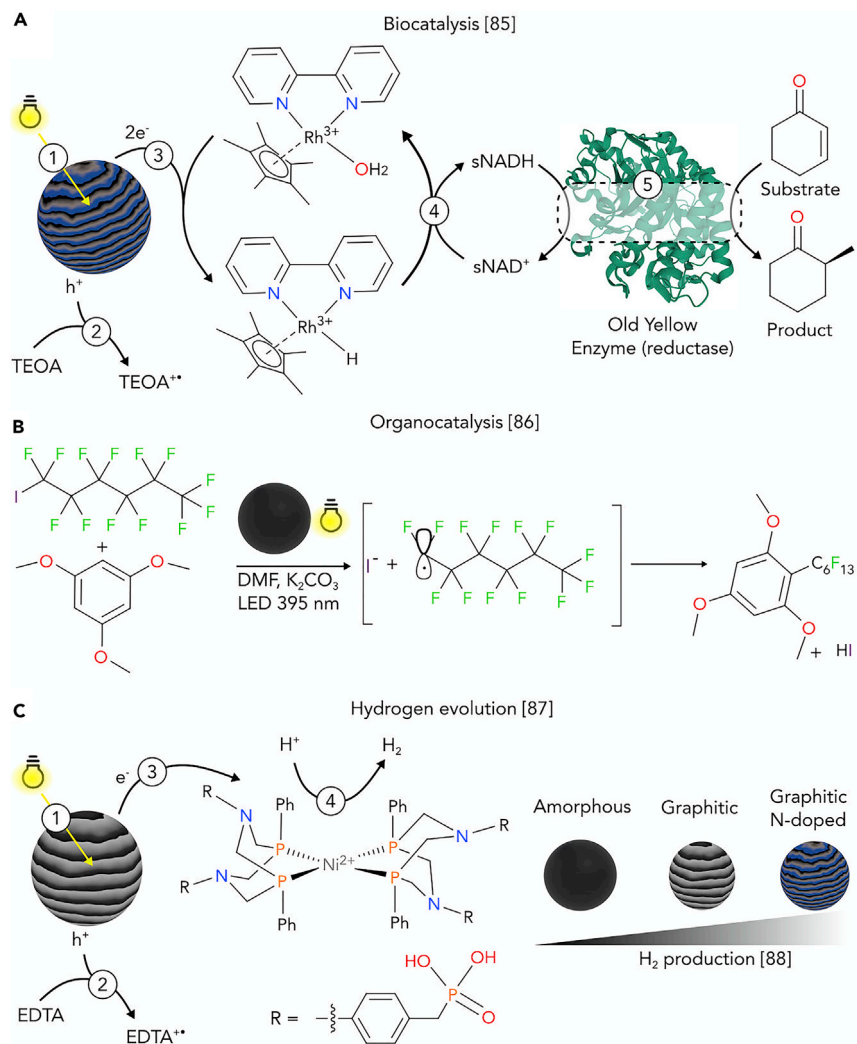


Figure 13. Photoinduced catalytic processes

(A) Steps involved in the biocatalytic asymmetric hydrogenation promoted by CNCs and mediated by an Rh(III) organometallic complex.

(B) Perfluoroalkylation reaction enabled by CNCs.

(C) Steps involved in the catalytic hydrogen evolution promoted by CNCs and mediated by a Ni(diphosphine)₂ catalyst; the trend in photocatalytic activity for different CNCs is also illustrated.

Universities, MICIU (project PID2019-108523RB-I00); the Ministry of Science and Higher Education of the Russian Federation (grant 14.Y26.31.0028); the Research Grant Council of Hong Kong SAR (CityU 11306619); and the Science Technology and Innovation Committee of Shenzhen Municipality (JCYJ20190808181201899). The major funding for this work to N.A.K. was provided by the Vannewar Bush DoD Fellowship titled "Engineered Chiral Ceramics" ONR N000141812876. A part of this work was supported by the NSF projects #1463474 titled "Energy- and Cost-Efficient Manufacturing Employing Nanoparticles" and #566460 titled "Nanospiked Particles for Photocatalysis." This work was performed under the Maria de Maeztu Units of Excellence Program from the Spanish State Research Agency grant no.MDM-2017-0720. We acknowledge support by the Deutsche Forschungsgemeinschaft (DFG) via SFB 953 "Synthetic Carbon Allotropes". G.R. thanks Dr. Luca Ravotto and Dr. Jacopo Tessarolo for fruitful discussions.

DECLARATION OF INTERESTS

D.M.G. is a member of the advisory board of Chem.

REFERENCES

1. Baker, S.N., and Baker, G.A. (2010). Luminescent carbon nanodots: emergent nanolights. *Angew Chem Int Ed Engl* 49, 6726–6744.
2. Lim, S.Y.Y., Shen, W., and Gao, Z. (2015). Carbon quantum dots and their applications. *Chem. Soc. Rev.* 44, 362–381.
3. Sun, Y.-P. (2020). *Carbon Dots* (Springer Nature).
4. Xiong, Y., Schneider, J., Ushakova, E.V., and Rogach, A.L. (2018). Influence of molecular fluorophores on the research field of chemically synthesized carbon dots. *Nano Today* 23, 124–139.
5. Sciortino, A., Cannizzo, A., and Messina, F. (2018). Carbon nanodots: a review—from the current understanding of the fundamental photophysics to the full control of the optical response. *C* 4, 67.
6. Demchenko, A. (2019). Excitons in carbonic nanostructures. *C* 5, 71.
7. Xia, C., Zhu, S., Feng, T., Yang, M., and Yang, B. (2019). Evolution and synthesis of carbon dots: from carbon dots to carbonized polymer dots. *Adv Sci (Weinh)* 6, 1901316.
8. de Medeiros, T.V.V., Manioudakis, J., Noun, F., Macairan, J.-R., Victoria, F., and Naccache, R. (2019). Microwave-assisted synthesis of carbon dots and their applications. *J. Mater. Chem. C* 7, 7175–7195.
9. Essner, J.B.B., Kist, J.A.A., Polo-Parada, L., and Baker, G.A.A. (2018). Artifacts and errors associated with the ubiquitous presence of fluorescent impurities in carbon nanodots. *Chem. Mater.* 30, 1878–1887.
10. Khan, S., Sharma, A., Ghoshal, S., Jain, S., Hazra, M.K., and Nandi, C.K. (2018). Small molecular organic nanocrystals resemble carbon nanodots in terms of their properties. *Chem. Sci.* 9, 175–180.
11. Qu, Z.B., Feng, W.J., Wang, Y., Romanenko, F., and Kotov, N.A. (2020). Diverse nanoassemblies of graphene quantum dots and their mineralogical counterparts. *Angew. Chem. Int. Ed. Engl.* 59, 8542–8551.
12. Sudolská, M., Dubecký, M., Sarkar, S., Reckmeier, C.J., Zbořil, R., Rogach, A.L., and Otyepka, M. (2015). Nature of absorption bands in oxygen-functionalized graphitic carbon dots. *J. Phys. Chem. C* 119, 13369–13373.
13. Holá, K., Sudolská, M., Kalytchuk, S., Nachtigallová, D., Rogach, A.L., Otyepka, M., and Zbořil, R. (2017). Graphitic nitrogen triggers red fluorescence in carbon dots. *ACS Nano* 11, 12402–12410.
14. Cao, L., Wang, X., Mezziani, M.J., Lu, F., Wang, H., Luo, P.G., Lin, Y., Harruff, B.A., Veca, L.M., Murray, D., et al. (2007). Carbon dots for multiphoton bioimaging. *J. Am. Chem. Soc.* 129, 11318–11319.
15. Li, D., Jing, P., Sun, L., An, Y., Shan, X., Lu, X., Zhou, D., Han, D., Shen, D., Zhai, Y., et al. (2018). Near-infrared excitation/emission and multiphoton-induced fluorescence of carbon dots. *Adv. Mater.* 30, e1705913.
16. Lan, M., Zhao, S., Zhang, Z., Yan, L., Guo, L., Niu, G., Zhang, J., Zhao, J., Zhang, H., Wang, P., et al. (2017). Two-photon-excited near-infrared emissive carbon dots as multifunctional agents for fluorescence imaging and photothermal therapy. *Nano Res* 10, 3113–3123.
17. Lu, S., Sui, L., Liu, J., Zhu, S., Chen, A., Jin, M., and Yang, B. (2017). Near-infrared photoluminescent polymer-carbon nanodots with two-photon fluorescence. *Adv. Mater.* 29, 1603443.
18. Jiang, L., Ding, H., Xu, M., Hu, X., Li, S., Zhang, M., Zhang, Q., Wang, Q., Lu, S., Tian, Y., and Bi, H. (2020). UV-vis-NIR full-range responsive carbon dots with large multiphoton absorption cross sections and deep-red fluorescence at nucleoli and in vivo. *Small* 16, e2000680.
19. Guerrero-Martínez, A., Alonso-Gómez, J.L., Auguie, B., Cid, M.M., and Liz-Marzán, L.M. (2011). From individual to collective chirality in metal nanoparticles. *Nano Today* 6, 381–400.
20. Ru, Y., Ai, L., Jia, T., Liu, X., Lu, S., Tang, Z., and Yang, B. (2020). Recent advances in chiral carbonized polymer dots: from synthesis and properties to applications. *Nano Today* 34, 100953.
21. Đorđević, L., Arcudi, F., D'Urso, A., Cacioppo, M., Micali, N., Bürgi, T., Purrello, R., and Prato, M. (2018). Design principles of chiral carbon nanodots help convey chirality from molecular to nanoscale level. *Nat. Commun.* 9, 3442.
22. Suzuki, N., Wang, Y., Elvati, P., Qu, Z.-B., Kim, K., Jiang, S., Baumeister, E., Lee, J., Yeom, B., Bahng, J.H., et al. (2016). Chiral graphene quantum dots. *ACS Nano* 10, 1744–1755.
23. Ma, W., Xu, L., De Moura, A.F., Wu, X., Kuang, H., Xu, C., and Kotov, N.A. (2017). Chiral inorganic nanostructures. *Chem. Rev.* 117, 8041–8093.
24. Peng, J., Gao, W., Gupta, B.K., Liu, Z., Romero-Aburto, R., Ge, L., Song, L., Alemany, L.B., Zhan, X., Gao, G., et al. (2012). Graphene quantum dots derived from carbon fibers. *Nano Lett* 12, 844–849.
25. Vázquez-Nakagawa, M., Rodríguez-Pérez, L., Herranz, M.A., and Martín, N. (2016). Chirality transfer from graphene quantum dots. *Chem. Commun.(Camb)*. 52, 665–668.
26. Vulugundam, G., Misra, S.K., Ostadhossein, F., Schwartz-Duval, A.S., Daza, E.A., and Pan, D. (2016). (-)/(+)-Sparteine induced chirally-active carbon nanoparticles for enantioselective separation of racemic mixtures. *Chem. Commun.(Camb)*. 52, 7513–7516.
27. Zhang, Y., Hu, L., Sun, Y., Zhu, C., Li, R., Liu, N., Huang, H., Liu, Y., Huang, C., and Kang, Z. (2016). One-step synthesis of chiral carbon quantum dots and their enantioselective recognition. *RSC Adv* 6, 59956–59960.
28. Đorđević, L., Arcudi, F., and Prato, M. (2019). Preparation, functionalization and characterization of engineered carbon nanodots. *Nat. Protoc.* 14, 2931–2953.
29. Di Mauro, A., Randazzo, R., Spanò, S.F., Compagnini, G., Gaeta, M., D'Urso, L., Paolesse, R., Pomarico, G., Di Natale, C., Villari, V., et al. (2016). Vortexes tune the chirality of graphene oxide and its non-covalent hosts. *Chem. Commun.(Camb)* 52, 13094–13096.
30. Kim, Y., Yeom, B., Arteaga, O., Jo Yoo, S.J., Lee, S.G., Kim, J.G., and Kotov, N.A. (2016). Reconfigurable chiroptical nanocomposites with chirality transfer from the macro- to the nanoscale. *Nat. Mater.* 15, 461–468.
31. Chekini, M., Prince, E., Zhao, L., Mundoor, H., Smalyukh, I.I., and Kumacheva, E. (2019). Chiral carbon dots synthesized on cellulose nanocrystals. *Adv. Opt. Mater.* 8, 1901911.
32. Shamsipur, M., Barati, A., Taherpour, A.A., and Jamshidi, M. (2018). Resolving the multiple emission centers in carbon dots: From fluorophore molecular states to aromatic domain states and carbon-core states. *J. Phys. Chem. Lett.* 9, 4189–4198.
33. Tao, S., Zhu, S., Feng, T., Zheng, C., and Yang, B. (2020). Crosslink-enhanced emission effect on luminescence in polymers: advances and perspectives. *Angew. Chem. Int. Ed. Engl.* 59, 9826–9840.
34. Tao, S., Song, Y., Zhu, S., Shao, J., and Yang, B. (2017). A new type of polymer carbon dots with high quantum yield: From synthesis to investigation on fluorescence mechanism. *Polymer* 116, 472–478.
35. Schneider, J., Reckmeier, C.J., Xiong, Y., Von Seckendorff, M., Susha, A.S., Kasák, P., and Rogach, A.L. (2017). Molecular fluorescence in citric acid-based carbon dots. *J. Phys. Chem. C* 121, 2014–2022.
36. Vallan, L., Urriolaibeitia, E.P., Ruipérez, F., Matxain, J.M., Canton-Vitoria, R., Tagmatarchis, N., Benito, A.M., and Maser, W.K. (2018). Supramolecular-enhanced charge transfer within entangled polyamide chains as the origin of the universal blue fluorescence of polymer carbon dots. *J. Am. Chem. Soc.* 140, 12862–12869.
37. Song, Y., Zhu, S., Zhang, S., Fu, Y., Wang, L., Zhao, X., and Yang, B. (2015). Investigation from chemical structure to photoluminescent mechanism: a type of carbon dots from the pyrolysis of citric acid and an amine. *J. Mater. Chem. C* 3, 5976–5984.
38. Shao, J., Zhu, S., Liu, H., Song, Y., Tao, S., and Yang, B. (2017). Full-color emission polymer carbon dots with quench-resistant solid-state fluorescence. *Adv Sci (Weinh)* 4, 1700395.

39. Krysmann, M.J., Kellarakis, A., Dallas, P., and Giannelis, E.P. (2012). Formation mechanism of carbogenic nanoparticles with dual photoluminescence emission. *J. Am. Chem. Soc.* 134, 747–750.
40. Fu, M., Ehrat, F., Wang, Y., Milowska, K.Z., Reckmeier, C., Rogach, A.L., Stolarczyk, J.K., Urban, A.S., and Feldmann, J. (2015). Carbon dots: a unique fluorescent cocktail of polycyclic aromatic hydrocarbons. *Nano Lett* 15, 6030–6035.
41. Yuan, F., Yuan, T., Sui, L., Wang, Z., Xi, Z., Li, Y., Li, X., Fan, L., Tan, Z., Chen, A., et al. (2018). Engineering triangular carbon quantum dots with unprecedented narrow bandwidth emission for multicolored LEDs. *Nat. Commun.* 9, 2249.
42. Sk, M.A., Ananthanarayanan, A., Huang, L., Lim, K.H., and Chen, P. (2014). Revealing the tunable photoluminescence properties of graphene quantum dots. *J. Mater. Chem. C* 2, 6954–6960.
43. Yan, F., Bai, Z., Zu, F., Zhang, Y., Sun, X., Ma, T., and Chen, L. (2019). Yellow-emissive carbon dots with a large Stokes shift are viable fluorescent probes for detection and cellular imaging of silver ions and glutathione. *Microchim. Acta* 186, 113.
44. Liu, H., Li, Z., Sun, Y., Geng, X., Hu, Y., Meng, H., Ge, J., and Qu, L. (2018). Synthesis of luminescent carbon dots with ultrahigh quantum yield and inherent folate receptor-positive cancer cell targetability. *Sci. Rep.* 8, 1086.
45. Yan, F., Jiang, Y., Sun, X., Bai, Z., Zhang, Y., and Zhou, X. (2018). Surface modification and chemical functionalization of carbon dots: a review. *Microchim. Acta* 185, 424.
46. Li, L., and Dong, T. (2018). Photoluminescence tuning in carbon dots: surface passivation or/and functionalization, heteroatom doping. *J. Mater. Chem. C* 6, 7944–7970.
47. Wang, Y., Meng, H., Jia, M., Zhang, Y., Li, H., and Feng, L. (2016). Intraparticle FRET of Mn(II)-doped carbon dots and its application in discrimination of volatile organic compounds. *Nanoscale* 8, 17190–17195.
48. Shi, X., Meng, H., Sun, Y., Qu, L., Lin, Y., Li, Z., and Du, D. (2019). Far-red to near-infrared carbon dots: preparation and applications in biotechnology. *Small* 15, e1901507.
49. Liu, J.J., Li, D., Zhang, K., Yang, M., Sun, H., and Yang, B. (2018). One-step hydrothermal synthesis of nitrogen-doped conjugated carbonized polymer dots with 31% efficient red emission for in vivo imaging. *Small* 14, e1703919.
50. Ding, H., Wei, J.S., Zhong, N., Gao, Q.Y., and Xiong, H.M. (2017). Highly efficient red-emitting carbon dots with gram-scale yield for bioimaging. *Langmuir* 33, 12635–12642.
51. Wang, L., Zhu, S.J., Wang, H.Y., Wang, Y.F., Hao, Y.W., Zhang, J.H., Chen, Q.D., Zhang, Y.L., Han, W., Yang, B., and Sun, H.-B. (2013). Unraveling bright molecule-like state and dark intrinsic state in green-fluorescence graphene quantum dots via ultrafast spectroscopy. *Advanced Optical Materials* 1, 264–271.
52. Das, A., Roy, D., De, C.K., and Mandal, P.K. (2018). "Where does the fluorescing moiety reside in a carbon dot?"—investigations based on fluorescence anisotropy decay and resonance energy transfer dynamics. *Phys. Chem. Chem. Phys.* 20, 2251–2259.
53. Righetto, M., Privitera, A., Fortunati, I., Mosconi, D., Zerbetto, M., Curri, M.L., Corricelli, M., Moretto, A., Agnoli, S., Franco, L., et al. (2017). Spectroscopic insights into carbon dot systems. *J. Phys. Chem. Lett.* 8, 2236–2242.
54. Righetto, M., Carraro, F., Privitera, A., Marafon, G., Moretto, A., and Ferrante, C. (2020). The elusive nature of carbon nanodot fluorescence: an unconventional perspective. *J. Phys. Chem. C* 124, 22314–22320.
55. Zhou, J., Chizhik, A.I., Chu, S., and Jin, D. (2020). Single-particle spectroscopy for functional nanomaterials. *Nature* 579, 41–50.
56. Ghosh, S., Chizhik, A.M., Karedla, N., Dekaliuk, M.O., Gregor, I., Schuhmann, H., Seibt, M., Bodensiek, K., Schaap, I.A.T., Schulz, O., et al. (2014). Photoluminescence of carbon nanodots: dipole emission centers and electron-phonon coupling. *Nano Lett* 14, 5656–5661.
57. Nguyen, H.A., Srivastava, I., Pan, D., and Gruebele, M. (2020). Unraveling the fluorescence mechanism of carbon dots with sub-single-particle resolution. *ACS Nano* 14, 6127–6137.
58. Bao, L., Liu, C., Zhang, Z.L., and Pang, D.W. (2015). Photoluminescence-tunable carbon nanodots: surface-state energy-gap tuning. *Adv. Mater.* 27, 1663–1667.
59. Das, S.K., Liu, Y., Yeom, S., Kim, D.Y., and Richards, C.I. (2014). Single-particle fluorescence intensity fluctuations of carbon nanodots. *Nano Lett* 14, 620–625.
60. Verma, N.C., Rao, C., and Nandi, C.K. (2018). Nitrogen-doped biocompatible carbon dot as a fluorescent probe for Storm nanoscopy. *J. Phys. Chem. C* 122, 4704–4709.
61. Baroncini, M., Bergamini, G., and Ceroni, P. (2017). Rigidification or interaction-induced phosphorescence of organic molecules. *Chem. Commun.(Camb)* 53, 2081–2093.
62. Jiang, K., Wang, Y., Li, Z., and Lin, H. (2020). Afterglow of carbon dots: mechanism, strategy and applications. *Mater. Chem. Front.* 4, 386–399.
63. Li, Q., Zhou, M., Yang, M., Yang, Q., Zhang, Z., and Shi, J. (2018). Induction of long-lived room temperature phosphorescence of carbon dots by water in hydrogen-bonded matrices. *Nat. Commun.* 9, 734.
64. Tao, S., Lu, S., Geng, Y., Zhu, S., Redfern, S.A.T., Song, Y., Feng, T., Xu, W., and Yang, B. (2018). Design of metal-free polymer carbon dots: a new class of room-temperature phosphorescent materials. *Angew. Chem. Int. Ed. Engl.* 57, 2393–2398.
65. Xia, C., Tao, S., Zhu, S., Song, Y., Feng, T., Zeng, Q., Liu, J., and Yang, B. (2018). Hydrothermal addition polymerization for ultrahigh-yield carbonized polymer dots with room temperature phosphorescence via nanocomposite. *Chemistry* 24, 11303–11308.
66. Jiang, K., Wang, Y., Gao, X., Cai, C., and Lin, H. (2018). Facile, quick, and gram-scale synthesis of ultralong-lifetime room-temperature-phosphorescent carbon dots by microwave irradiation. *Angew. Chem. Int. Ed. Engl.* 57, 6216–6220.
67. Wang, Z., Liu, Y., Zhen, S., Li, X., Zhang, W., Sun, X., Xu, B., Wang, X., Gao, Z., and Meng, X. (2020). Gram-scale synthesis of 41% efficient single-component white-light-emissive carbonized polymer dots with hybrid fluorescence/phosphorescence for white light-emitting diodes. *Adv Sci (Weinh)* 7, 1902688.
68. Jiang, K., Wang, Y., Cai, C., and Lin, H. (2017). Activating room temperature long afterglow of carbon dots via covalent fixation. *Chem. Mater.* 29, 4866–4873.
69. Efremushkin, L., Bhunia, S.K., Jelinek, R., and Salomon, A. (2017). Carbon dots–plasmonics coupling enables energy transfer and provides unique chemical signatures. *J. Phys. Chem. Lett.* 8, 6080–6085.
70. Li, M., Chen, T., Gooding, J.J., and Liu, J. (2019). Review of carbon and graphene quantum dots for sensing. *ACS Sens* 4, 1732–1748.
71. Kim, Y., Jang, G., and Lee, T.S. (2015). New fluorescent metal-ion detection using a paper-based sensor strip containing tethered rhodamine carbon nanodots. *ACS Appl. Mater. Interfaces* 7, 15649–15657.
72. Khakbaz, F., and Mahani, M. (2017). Micro-RNA detection based on fluorescence resonance energy transfer of DNA-carbon quantum dots probes. *Anal. Biochem.* 523, 32–38.
73. Strauss, V., Margraf, J.T., Dolle, C., Butz, B., Nacken, T.J., Walter, J., Bauer, W., Peukert, W., Spiecker, E., Clark, T., and Guldi, D.M. (2014). Carbon nanodots: toward a comprehensive understanding of their photoluminescence. *J. Am. Chem. Soc.* 136, 17308–17316.
74. Cailotto, S., Mazzaro, R., Enrichi, F., Vomiero, A., Selva, M., Cattaruzza, E., Cristofori, D., Amadio, E., and Perosa, A. (2018). Design of carbon dots for metal-free photoredox catalysis. *ACS Appl. Mater. Interfaces* 10, 40560–40567.
75. Arcudi, F., Strauss, V., Đorđević, L., Cadranel, A., Guldi, D.M.M., and Prato, M. (2017). Porphyrin antennas on carbon nanodots: excited state energy and electron transduction. *Angew. Chem. Int. Ed. Engl.* 56, 12097–12101.
76. Cacioppo, M., Scharl, T., Đorđević, L., Cadranel, A., Arcudi, F., Guldi, D.M., and Prato, M. (2020). Symmetry-breaking charge transfer chromophore interactions supported by carbon-nanodots. *Angew. Chem. Int. Ed. Engl.* 59, 12779–12784.
77. Strauss, V., Margraf, J.T., Dirian, K., Syrgiannis, Z., Prato, M., Wessendorf, C., Hirsch, A., Clark, T., and Guldi, D.M. (2015). Carbon nanodots: supramolecular electron donor-acceptor hybrids featuring Peryleneimides. *Angew. Chem. Int. Ed. Engl.* 54, 8292–8297.
78. Barman, M.K., Jana, B., Bhattacharyya, S., and Patra, A. (2014). Photophysical properties of doped carbon dots (N, P, and B) and their influence on electron/hole transfer in carbon dots-nickel (II) phthalocyanine conjugates. *J. Phys. Chem. C* 118, 20034–20041.

79. Hutton, G.A.M., Martindale, B.C.M., and Reisner, E. (2017). Carbon dots as photosensitisers for solar-driven catalysis. *Chem. Soc. Rev.* *46*, 6111–6123.
80. Yang, P., Zhao, J., Wang, J., Cui, H., Li, L., and Zhu, Z. (2015). Pure carbon nanodots for excellent photocatalytic hydrogen generation. *RSC Adv* *5*, 21332–21335.
81. Yang, P., Zhao, J., Wang, J., Cui, H., Li, L., and Zhu, Z. (2015). Multifunctional nitrogen-doped carbon nanodots for photoluminescence, sensor, and visible-light-induced H₂ production. *ChemPhysChem* *16*, 3058–3063.
82. Bhattacharyya, S., Ehrat, F., Urban, P., Teves, R., Wyrwich, R., Döblinger, M., Feldmann, J., Urban, A.S., and Stolarczyk, J.K. (2017). Effect of nitrogen atom positioning on the trade-off between emissive and photocatalytic properties of carbon dots. *Nat. Commun.* *8*, 1401.
83. Hutton, G.A.M.M., Reuillard, B., Martindale, B.C.M.M., Caputo, C.A., Lockwood, C.W.J.J., Butt, J.N., and Reisner, E. (2016). Carbon dots as versatile photosensitizers for solar-driven catalysis with redox enzymes. *J. Am. Chem. Soc.* *138*, 16722–16730.
84. Kim, J., Lee, S.H., Tieves, F., Choi, D.S., Hollmann, F., Paul, C.E., and Park, C.B. (2018). Biocatalytic C=C bond reduction through carbon nanodot-sensitized regeneration of NADH analogues. *Angew. Chem. Int. Ed.* *57*, 13825–13828.
85. Rosso, C., Filippini, G., and Prato, M. (2019). Use of nitrogen-doped carbon nanodots for the photocatalytic fluoroalkylation of organic compounds. *Chemistry* *25*, 16032–16036.
86. Martindale, B.C.M., Hutton, G.A.M., Caputo, C.A., and Reisner, E. (2015). Solar hydrogen production using carbon quantum dots and a molecular nickel catalyst. *J. Am. Chem. Soc.* *137*, 6018–6025.
87. Martindale, B.C.M., Hutton, G.A.M., Caputo, C.A., Pranti, S., Godin, R., Durrant, J.R., and Reisner, E. (2017). Enhancing light absorption and charge transfer efficiency in carbon dots through graphitization and core nitrogen doping. *Angew. Chem. Int. Ed. Engl.* *56*, 6459–6463.
88. Choi, Y.Y., Jeon, D., Choi, Y.Y., Ryu, J., and Kim, B.S. (2018). Self-assembled supramolecular hybrid of carbon nanodots and polyoxometalates for visible-light-driven water oxidation. *ACS Appl. Mater. Interfaces* *10*, 13434–13441.
89. Zhang, P., Wang, T., Chang, X., Zhang, L., and Gong, J. (2016). Synergistic cocatalytic effect of carbon nanodots and Co₃O₄ nanoclusters for the photoelectrochemical water oxidation on hematite. *Angew. Chem. Int. Ed. Engl.* *55*, 5851–5855.
90. Wu, X., Zhao, J., Guo, S., Wang, L., Shi, W., Huang, H., Liu, Y., and Kang, Z. (2016). Carbon dot and BiVO₄ quantum dot composites for overall water splitting via a two-electron pathway. *Nanoscale* *8*, 17314–17321.
91. Melchiorre, P., Marigo, M., Carlone, A., and Bartoli, G. (2008). Asymmetric aminocatalysis - gold rush in organic chemistry. *Angew. Chem. Int. Ed. Engl.* *47*, 6138–6171.
92. Filippini, G., Amato, F., Rosso, C., Ragazzon, G., Vega-Peñalosa, A., Companyó, X., Dell'Amico, L., Bonchio, M., and Prato, M. (2020). Mapping the surface groups of amine-rich carbon dots enables covalent catalysis in aqueous media. *Chem* *6*, 3022–3037.
93. Li, S., Liu, J., Ramesar, N.S., Heinz, H., Xu, L., Xu, C., and Kotov, N.A. (2019). Single- and multi-component chiral supraparticles as modular enantioselective catalysts. *Nat. Commun.* *10*, 4826.